

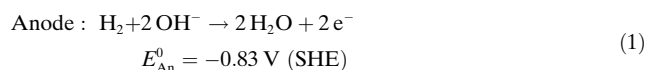
Hybrid Polymer Electrolyte Fuel Cells: Alkaline Electrodes with Proton Conducting Membrane

Murat Ünlü, Junfeng Zhou, and Paul A. Kohl*

Fuel cells have the potential to provide clean and efficient energy for stationary, traction, and portable applications.^[1] Among the various types of fuel cells, proton-exchange membrane (PEM) fuel cell has several desirable features including well established membranes and cell designs. Although PEM fuel cells have been used in numerous applications, there are several obstacles that impede wide-scale commercialization. These issues include the high cost of noble-metal catalysts and perfluorinated membranes, carbon monoxide poisoning, and limited lifetime due to membrane and electrode degradation.^[2–4]

Recently, there is a growing interest in anion-exchange membrane (AEM) fuel cells operating at high pH.^[5] The high-pH environment addresses many of the shortfalls experienced with PEM fuel cells. Alkaline cells can function with nickel and silver, and are resistant to CO poisoning.^[6,7] Although AEM fuel cells have several advantages compared to proton-based fuel cells, the lower ionic conductivity of AEMs compared to commercially available Nafion is a concern because it may lower the performance. Moreover, the strong dependence of the AEM conductivity on humidity and the need for water in the cathode reaction are significant challenges that limit the performance of current AEM fuel cells.^[8]

In an effort to use the high conductivity and established infrastructure of PEMs and still exploit the advantages of high-pH electrode operation—e.g., resistance to CO poisoning at the anode and use of non-platinum catalysts at the anode and cathode—we report here a hybrid fuel cell comprised of AEM electrodes and PEM core. The high-pH electrode (AEM electrode) was made using an anion-exchange ionomer (AEI), poly(aryleneether sulfone), functionalized with quaternary ammonium groups synthesized for this study, as described previously.^[9] The AEM electrodes were pressed onto a PEM membrane, Nafion212. The cell configuration is shown in Figure 1. Under alkaline conditions, the anode and cathode reactions are as follows:



[*] Dr. M. Ünlü, Dr. J. Zhou, Prof. Dr. P. A. Kohl
 School of Chemical and Biomolecular Engineering
 Georgia Institute of Technology
 Atlanta, Georgia 30332-0100 (USA)
 Fax: (+1) 404-894-2866
 E-mail: kohl@gatech.edu

Supporting information for this article is available on the WWW under <http://dx.doi.org/10.1002/anie.200906021>.

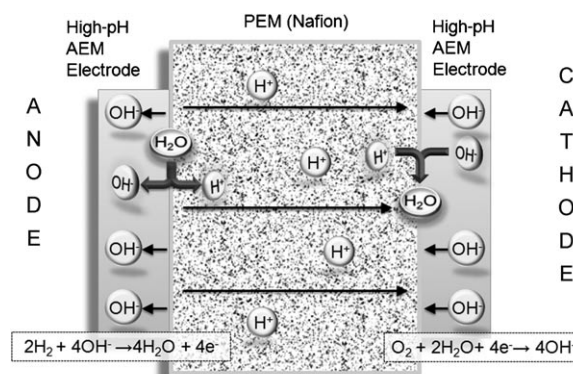
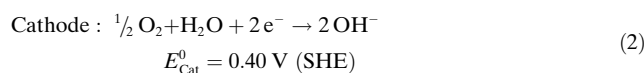


Figure 1. Operation mechanism of a hybrid fuel cell comprising high-pH AEM electrodes and a proton-conducting membrane.



A critical aspect of this AEM/PEM/AEM cell is the creation of two junctions formed at the interface between the proton conducting core membrane and alkaline electrodes. The electrochemical behavior of an AEM/PEM junction in an operating fuel cell has been evaluated.^[10] The junction potential created at the acid/alkaline boundary is described by Equation (3).

$$E_j = \phi^{\text{AEM}} - \phi^{\text{PEM}} = \frac{RT}{F} \ln \left(\frac{a_{\text{H}^+}^{\text{PEM}}}{a_{\text{H}^+}^{\text{AEM}}} \right) \quad (3)$$

The junction potentials are formed at the PEM/anode interface ($E_{j,\text{PEM}/\text{Ano}}$) and cathode/PEM interface ($E_{j,\text{Cat}/\text{PEM}}$) and constitute a perturbation to the Nernst potential. The junction potentials are defined as the potential difference between the AEM (ϕ^{AEM}) and the PEM phases (ϕ^{PEM}). Since these two junctions are in the opposite direction, the junction potentials cancel each other, resulting in a thermodynamic cell voltage of 1.23 V [Eqs. (4) and (5)].

$$\begin{aligned} E_{\text{cell}} &= E_{\text{Nernst}} + E_{j,\text{PEM}/\text{Ano}} + E_{j,\text{Cat}/\text{PEM}} \\ &= E_{\text{Nernst}} + (\phi^{\text{PEM}} - \phi^{\text{AEM}}) + (\phi^{\text{AEM}} - \phi^{\text{PEM}}) \end{aligned} \quad (4)$$

$$E_{\text{cell}} = 1.23 + \frac{RT}{2F} \ln \left[\frac{P_{\text{O}_2}^{1/2} P_{\text{H}_2}}{P_{\text{H}_2\text{O}}} \right] \quad (5)$$

The performance of the hybrid membrane electrode assembly (MEA) was evaluated for the H_2/O_2 system operating at 60°C. Both electrodes have a catalyst loading of 0.5 mg cm^{-2} Pt (20% by weight on carbon). The current–

voltage curves are shown in Figure 2 for 0 and 100% relative humidity (RH). At 100% RH, the open circuit potential was 976 mV, and the maximum power density was 55.6 mW cm⁻². Interestingly, the power density increased to 78.3 mW cm⁻²

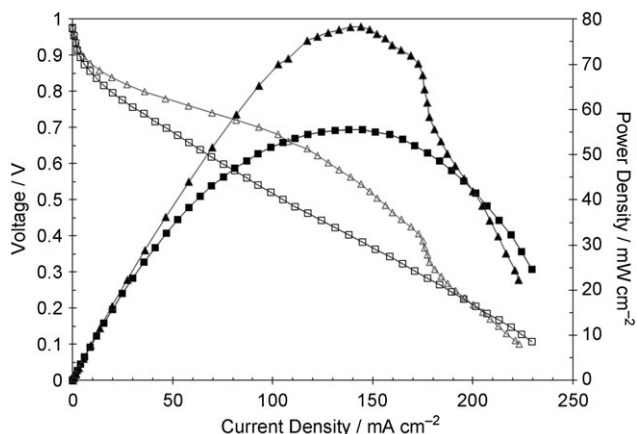


Figure 2. Polarization curves and power density of the hybrid cell at 60°C for 0 (triangles) and 100% (squares) RH levels. Catalyst loading is 0.5 mg cm⁻² Pt for both electrodes. Both H₂ and O₂ gas feeds are supplied at atmospheric pressure with flow rates of 6 and 8 s cm⁻³, respectively. Solid symbols correspond to power density.

when the cell was operated with dry gases. The increase in performance at lower RH is shown in Figure 3. The current density was recorded for each RH condition after 24 h of

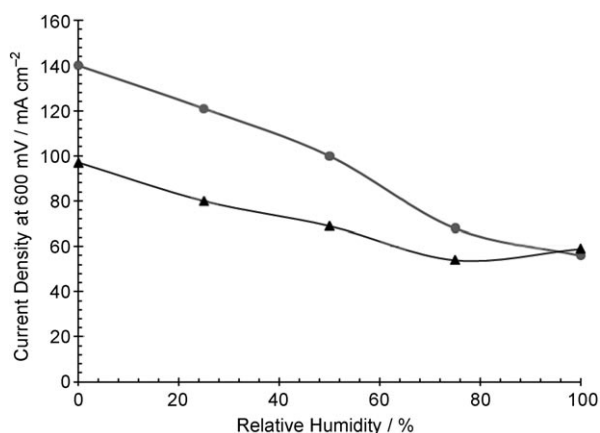
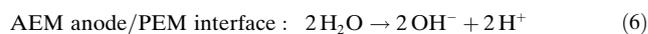


Figure 3. Current densities of the hybrid fuel cell at 600 mV as a function of RH for cell temperatures of 60 (▲) and 70°C (●). Both H₂ and O₂ gas feeds are supplied at atmospheric pressure with flow rates of 6 and 8 s cm⁻³, respectively.

operation at 600 mV corresponding to steady-state conditions. The current density was 59 mA cm⁻² at 100% RH while it was 97 mA cm⁻² at 0% RH. This behavior is in contrast to PEM and AEM fuel cells where high humidity is needed to achieve high performance. The increase in performance of the hybrid cells at lower RH is attributed to the superior water management configuration, as explained below.

In an operating hybrid cell, mobile OH⁻ ions within the AEM anode migrate away from the anode/PEM interface

toward the anode catalyst and the H⁺ migrates within the PEM toward the PEM/cathode interface, as depicted in Figure 1. As a result of migration, the AEM/PEM junction is depleted of OH⁻ and H⁺. This depletion region leads to a junction potential, $E_{j,PEM/Ano}$, as defined above. Water dissociation occurs at the interface [Eq. (6)]:^[11,12]



Protons within the PEM migrate towards the PEM/cathode interface, and hydroxide in the cathode layer migrates towards the PEM/cathode junction. Recombination of the proton and hydroxide forms water at the junction [Eq. (7)]:



It is of particular interest that water is generated at two points within the MEA: 1) within the anode layer and 2) at the PEM/cathode junction. This is contrary to a traditional PEM fuel cell where water is generated at the cathode (product of oxygen reduction). Typically, PEM fuel cells lose performance when dry gas feed conditions are used due to dry-out, especially within the anode layer. For the AEM fuel cell, water is formed within the anode layer and consumed at the cathode. The unique water management in the hybrid cell enables self-hydrating of the MEA at dry conditions because water is formed near to where it is consumed. Currently, the hybrid cell operates steadily at 70°C with dry gas feeds and the current density of 150 mA cm⁻² for several days (see Figure S1 in the Supporting Information).

To assist in understanding the characteristics of the operating hybrid cell, AC impedance spectroscopy was used to diagnose the impedance of the cell components. Figure 4 shows impedance spectra collected at a cell voltage of 600 mV for different gas RH values at 60°C. The spectra are semicircle loops at all cell conditions. Typically, the difference between the x intercept values at high and low frequency corresponds to the charge transfer resistance at the electrode, and the high-frequency x intercept (R_{HF}) corresponds to the MEA ionic resistance. For the fully humidified cell, R_{HF} is 198 mΩ cm². This low ionic resistance is a clear sign that the

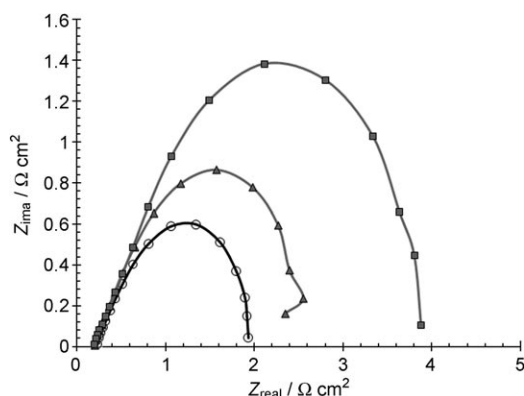


Figure 4. In situ AC impedance spectra of the hybrid fuel cell at 600 mV and 60°C for 0 (○), 50 (△), and 100% (□) humidification levels.

Nafion core is being used in its fully conductive form, which is one of the goals of this study. For comparison, this internal resistance is significantly lower than the value of $460 \text{ m}\Omega \text{ cm}^2$ for the recently developed AEM fuel cell.^[13]

Impedance data shows that the ionic resistance of the membrane remained nearly constant as a function of the feed gas RH, as shown in Figure 4. This observation is an indication that the water generated at the PEM/cathode interface and at the anode, see Figure 1, hydrates the MEA even under dry feed gas conditions. However, the charge transfer resistance (difference between the two x intercepts of the impedance loop at high and low frequency) increased at higher feed gas RH. The effective charge transfer resistance is mainly determined by interfacial reaction kinetics, and ionic conductivity and diffusion limitations within the catalyst layer.^[14] The likely cause of the greater resistance at high RH is from limited diffusion within the catalyst layer and not the PEM since the ionic conductivity of the PEM does not decrease. In our previous report, the flooding within the catalyst layer was shown to be the primary reason for this mass transfer limitation.^[15] Further experimental work is needed to confirm if this limitation is indeed due to flooding within the electrodes. In traditional PEM fuel cells, the charge transfer resistance is assigned primarily to the cathode reaction because the anode overpotential is negligible compared to the cathode overpotential.^[16] Since the mass transfer dynamics of the hybrid cell anode is significantly altered, the individual effect of the anode and cathode on the AC impedance spectra should be considered. Further characterizations are underway to distinguish between the contributions of the two electrodes in the performance of the hybrid cell.

In summary, the viability of the hybrid fuel cell comprised of alkaline electrodes and PEM core was demonstrated. The AEM/PEM junction between AEM electrodes and the PEM core introduces an additional perturbation to the Nernst voltage. The bias direction depends on the direction of the electric field. Since the two junctions of the AEM/PEM/AEM cell have opposite fields, their junction potentials cancel each other, resulting in a thermodynamic cell voltage of 1.23 V for a hydrogen/oxygen cell. Significantly, water management is enhanced compared to traditional PEM and AEM fuel cells. This study addresses several of the major challenges in low-temperature fuel-cell technology, including utilization of non-precious catalysts, simplified water management, and resistance to CO poisoning. Further innovations for liquid-feed fuel cells are also possible. The improved performance and possibility of using alternate liquid fuels may be possible because the oxidation of electroactive hydrocarbons is more facile in alkaline environments than in acid environments.

Experimental Section

The high-pH electrode (AEM electrode) was made using an anion-exchange ionomer (AEI), poly(aryleneether sulfone) functionalized with quaternary ammonium groups synthesized for this study, as described previously.^[9] The physical properties of the AEM are summarized in Table 1. The AEI was stored as a solution of 5% mass in dimethyl formamide (DMF). The Nafion membranes were pre-treated with 3% H_2O_2 and 1M H_2SO_4 solutions.

Table 1: Physical properties of the AEM membrane used in this study.^[a]

ionic functional group	$-\text{N}^+(\text{CH}_3)_3\text{OH}^-$
conductivity [mS cm^{-1}]	21.2
water uptake [%]	63.9
ion-exchange capacity [mmol g^{-1}]	1.77 ± 0.08
density [g cm^{-3}]	1.24 ± 0.01

[a] All measurements were performed at room temperature.

The catalyst ink for the anionic, high-pH electrode was prepared by mixing the Pt/C catalyst and the AEI with a mixture of water and DMF (2:3 by mass). The catalyst inks were sonicated for 15 min and then cast onto hydrophobic Toray carbon paper (TGPH-090). The resulting electrodes had a surface area of 2 cm^2 and catalyst loading of 0.5 mg cm^{-2} .

Initially, 50 μL of AEI in DMF (1% mass) was sprayed directly onto the surface of the AEM electrode. After drying at room temperature, the AEM electrodes were immersed in aqueous 0.1M KOH to exchange OH^- for Cl^- . 100 μL of Nafion (5% suspension): IPA mixture (1:2 by volume) was sprayed onto both the AEM electrodes before assembling the electrodes onto the membrane. The AEM electrodes were pressed onto Nafion 212 at 2 MPa and ambient temperature for 3 min. All MEAs were preconditioned by operating them in a fuel cell at steady state at 600 mV discharge voltage for 24 h before performing I - V polarization experiments. Electrochemical measurements were performed using a PAR 2273 potentiostat/galvanostat. Fuel cell tests were conducted at ambient pressure. Electrochemical impedance spectra were measured, following polarization curves, in the constant voltage mode using frequencies from 10 mHz–10 kHz. The amplitude of the AC voltage was 10 mV.

Received: October 26, 2009

Published online: January 18, 2010

Keywords: alkaline electrodes · fuel cells · hybrid materials · ionic conductivity · proton-exchange membrane

- [1] J. Larminie, A. Dicks, *Fuel Cell Systems Explained*, 2nd ed., Wiley, Chichester, **2003**.
- [2] T. V. Nguyen, R. E. White, *J. Electrochem. Soc.* **1993**, *140*, 2178.
- [3] J.-H. Wee, K.-Y. Lee, *J. Power Sources* **2006**, *157*, 128.
- [4] K. Yasuda, A. Taniguchi, T. Akita, T. Ioroi, Z. Siroma, *Phys. Chem. Chem. Phys.* **2006**, *8*, 746.
- [5] J. R. Varcoe, R. C. T. Slade, *Fuel Cells* **2005**, *5*, 187.
- [6] J. R. Varcoe, R. C. T. Slade, G. L. Wright, Y. Chen, *J. Phys. Chem. B* **2006**, *110*, 21041.
- [7] J. S. Spendlow, J. D. Goodpaster, P. J. A. Kenis, A. Wieckowski, *J. Phys. Chem. B* **2006**, *110*, 9545.
- [8] C. Tamain, S. D. Poynton, R. C. T. Slade, B. Carroll, J. R. Varcoe, *J. Phys. Chem. C* **2007**, *111*, 18423.
- [9] J. Zhou, M. Ünlü, J. A. Vega, P. A. Kohl, *J. Power Sources* **2009**, *190*, 285.
- [10] M. Ünlü, J. Zhou, P. A. Kohl, *J. Phys. Chem. C* **2009**, *113*, 11416.
- [11] H. D. Hurwitz, R. Dibiani, *Electrochim. Acta* **2001**, *47*, 759.
- [12] H. Strathmann, H. J. Rapp, B. Bauer, C. M. Bell, *Desalination* **1993**, *90*, 303.
- [13] S. Gu, R. Cai, T. Luo, Z. Chen, M. Sun, Y. Liu, G. He, Y. Yan, *Angew. Chem.* **2009**, *121*, 6621; *Angew. Chem. Int. Ed.* **2009**, *48*, 6499.
- [14] T. E. Springer, T. A. Zawodzinski, M. S. Wilson, S. Gottesfeld, *J. Electrochem. Soc.* **1996**, *143*, 587.
- [15] M. Ünlü, J. Zhou, P. A. Kohl, *Fuel Cells* **2009**, DOI: 10.1002/fuce200900122.
- [16] M. Ciureanu, H. Wang, *J. Electrochem. Soc.* **1999**, *146*, 4031.